

Magnetotransport in Two-Dimensional Electron Systems with Spin-Orbit Interaction

M. Langenbuch,* M. Suhrke,† and U. Rössler

Institut für Theoretische Physik - Universität Regensburg, 93040 Regensburg, Germany

(Dated: October 31, 2018)

We present magnetotransport calculations for homogeneous two-dimensional electron systems including the Rashba spin-orbit interaction, which mixes the spin-eigenstates and leads to a modified fan-chart with crossing Landau levels. The quantum mechanical Kubo formula is evaluated by taking into account spin-conserving scatterers in an extension of the self-consistent Born approximation that considers the spin degree of freedom. The calculated conductivity exhibits besides the well-known beating in the Shubnikov-de Haas (SdH) oscillations a modulation which is due to a suppression of scattering away from the crossing points of Landau levels and does not show up in the density of states. This modulation, surviving even at elevated temperatures when the SdH oscillations are damped out, could serve to identify spin-orbit coupling in magnetotransport experiments. Our magnetotransport calculations are extended also to lateral superlattices and predictions are made with respect to $1/B$ periodic oscillations in dependence on carrier density and strength of the spin-orbit coupling.

PACS numbers: 72.20.-i;73.23.-b;85.75.-d

Keywords: spin-orbit interaction; magnetotransport

I. INTRODUCTION

The Rashba spin-orbit coupling^{1,2} that exists in systems with axial symmetry, plays a key role in spintronics³ realized with two-dimensional (2D) carriers in semiconductor heterostructures as it allows to manipulate the spin by a gate-controlled confinement potential. Spin-orbit (SO) coupling mixes the spin states and removes the spin degeneracy for states with finite momentum. Besides the Rashba term caused by the asymmetry of the confinement, there exists also a SO coupling due to the inversion asymmetry of the crystalline structure of the semiconductor bulk material (Dresselhaus term⁴). Both types of SO coupling combine to an anisotropic spin-splitting of 2D electrons, which has been analyzed by inelastic light scattering⁵ and play a role also in weak localization studies^{6,7}. The intimate relation between spin splitting and spin relaxation, well-known for bulk material^{8,9} has found renewed interest for 2D electrons^{10,11}, furthered by the possibility to measure spin-relaxation times with monopolar optical orientation¹². The zero-field spin splitting¹³ has to compete with the Zeeman spin-splitting if a magnetic field is applied perpendicular to the plane of the 2D electron system. This results in a fan chart showing characteristic crossings of Landau levels, which in magnetotransport data are detected as beating of the Shubnikov de-Haas (SdH) oscillations^{14,15,16,17}. For hole systems, the two SO coupling mechanisms have been found to be responsible for anomalous SdH oscillations^{18,19}. The structural asymmetry of the confinement can be tuned into a regime where the Rashba SO coupling dominates over the bulk inversion asymmetry¹³. In spite of this current interest in the Rashba SO coupling and its relevance for spin-related transport in two-dimensional electron systems (2DES) it is surprising that there is so far no rigorous magnetotransport calculation which takes this coupling into ac-

count.

Here, we present fully quantum-mechanical calculations of the magnetoconductivity including the Rashba SO interaction. The calculations are based on the evaluation of the Kubo formula with an extension of the self-consistent Born approximation (SCBA) by taking into account the electron spin degree of freedom. Our results show besides the known beats in the SdH oscillations an additional modulation connected with the crossing of Landau levels. This modulation, which is not seen in the density of states, arises as we take into account spin-conserving impurity scattering which is suppressed when the SO coupled states are not degenerate. It survives even at higher temperatures, when SdH oscillations have died out, and could serve, if experimentally detected, as another fingerprint of SO interaction. In lateral superlattices²¹, where a 2DES is subjected to a periodic potential, there exist besides the SdH oscillations other $1/B$ periodic magnetotransport oscillations due to commensurability between cyclotron radius and lattice constant²² and due to the formation of a miniband structure^{23,24}. From our magnetotransport calculations for lateral superlattices with weak uni-directional (1D) modulation we predict a splitting of these periods due to SO coupling and calculate their dependence on its strength and carrier density.

The paper is organized in the following way. After this introduction we describe in the section II the energy spectrum and the eigenstates of a 2DES with Rashba SO interaction. For the calculation of the conductivity we simplify the energy spectrum and introduce a constant spin-splitting model. In the section III the SCBA is extended by the spin degree of freedom to describe the scattering of spin-conserving impurities in a 2DES with SO interaction. The effects of this extension are illustrated for a two level system, where it is shown that for non-degenerate SO coupled states the scattering efficiency is

suppressed. In section IV we present the conductivity and compare the cases with and without SO coupling. Finally in the section V we show results for a system with SO interaction and a 1D periodic modulation and study in the power spectrum of the magnetoconductivity the evolution of the characteristic periods with increasing SO coupling.

II. ENERGY SPECTRUM AND THE CONSTANT SPIN-ORBIT COUPLING MODEL

The Hamiltonian of a 2DES (in the xy -plane) realized in the lowest subband of a semiconductor heterostructure with effective mass m^* , Rashba SO interaction due to the z -confinement with coupling constant α_z , and Zeeman term with effective g -factor g^* , in a magnetic field $\mathbf{B} = B\hat{e}_z$, is given by

$$H = \frac{1}{2m^*} (\pi_x^2 + \pi_y^2) - \frac{\alpha_z}{\hbar} (\sigma_x \pi_y - \sigma_y \pi_x) + \frac{1}{2} g^* \mu_B \sigma_z B, \quad (1)$$

where π_μ denotes the kinetic momentum and σ_μ the Pauli spin matrices, $\mu \in \{x, y, z\}$. The spin (*up/down*) is quantized in z -direction. The energy spectrum is isotropic and without the magnetic field, $B = 0$, it depends on the wavevector \mathbf{k} and is given by¹

$$E_{\mathbf{k}}^\pm = \frac{\hbar^2 \mathbf{k}^2}{2m^*} \pm \alpha_z |\mathbf{k}|. \quad (2)$$

The SO coupling lifts the spin degeneracy even without external magnetic field and the energy branches are split by

$$\Delta_{\text{SO}} = 2\alpha_z |\mathbf{k}|. \quad (3)$$

Including the external magnetic field, the Hamiltonian can be formulated with ladder operators $a^\dagger |n\rangle = \sqrt{n+1} |n+1\rangle$, $a |n\rangle = \sqrt{n} |n-1\rangle$. In the Pauli representation the Hamiltonian can be written as

$$H = \hbar\omega_c \begin{pmatrix} a^\dagger a + \frac{1}{2} + \beta & \alpha a \\ \alpha a^\dagger & a^\dagger a + \frac{1}{2} - \beta \end{pmatrix}. \quad (4)$$

with the parameters $\beta = \frac{g^* \mu_B B}{2\hbar\omega_c}$ and $\alpha = -\frac{\alpha_z \sqrt{2}}{\lambda_c \hbar\omega_c}$, the cyclotron frequency $\omega_c = \frac{eB}{m^*}$ and the magnetic length $\lambda_c = \left(\frac{\hbar}{eB}\right)^{1/2}$.

In Fig. 1 we show the spectrum of Hamiltonian (1) without magnetic field (left) and with magnetic field (right) for parameter values corresponding to InAs ($m^* = 0.023 m_0$, $g^* = -14.9$). In Fig. 1a the situation without SO coupling with spin-degenerate parabolic dispersion (left) and regular fan-chart of Landau levels (right) is depicted. Including spin-orbit coupling the picture of Fig. 1b is obtained with the k -dependent splitting of the subband dispersion (left) and the characteristic crossing pattern of Landau levels (right). For this calculation the SO coupling parameter α_z was chosen to be

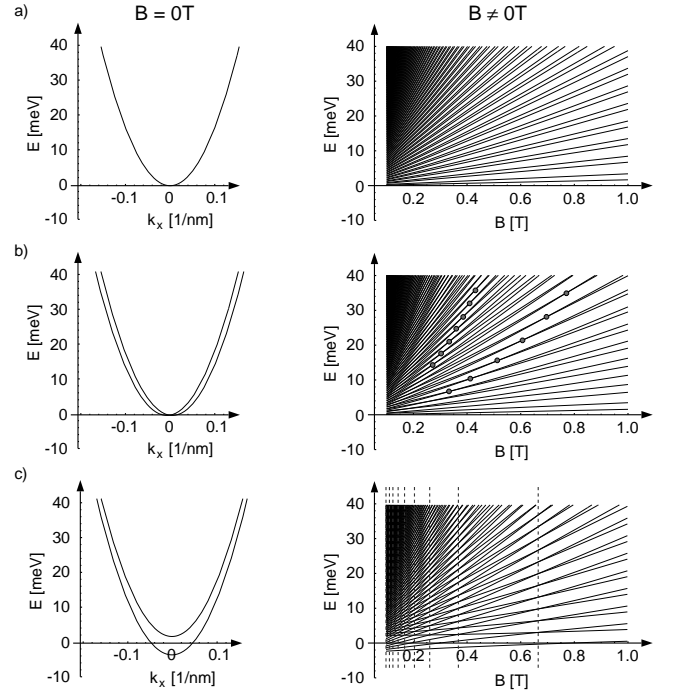


FIG. 1: Subband Energy dispersion (left) and Landau levels (right) of a 2DES (parameters $m^* = 0.023 m_0$, $g^* = -14.9$ correspond to InAs) a) without SO coupling $\alpha_z = 0$ eVm, b) with SO coupling $\alpha_z = 2.0 \times 10^{-11}$ eVm, and c) with constant spin-orbit splitting $\bar{\alpha}_z = 2.5$ meV.

$\alpha_z = 2.0 \times 10^{-11}$ eVm close to the experimental values reported for InAs samples¹⁴. The Hamiltonian (4) indicates that in the presence of SO coupling the spin states, quantized in z -direction and used in the Pauli representation, are no longer eigenstates. Instead Hamiltonian (4) is diagonal for the states¹

$$|n, r\rangle = \begin{pmatrix} c_{rn}^u \Phi_n \\ c_{rn}^d \Phi_{n+1} \end{pmatrix} \text{ and } |n, l\rangle = \begin{pmatrix} c_{ln}^u \Phi_{n-1} \\ c_{ln}^d \Phi_n \end{pmatrix} \quad (5)$$

which can be classified by the helicity $\kappa \in \{\text{right}, \text{left}\}$ and the Landau index $n = 0, 1, 2, \dots$. Φ_n are the eigenfunctions of the Landau oscillator. These *right/left* states evolve with increasing SO coupling from the spin *up/down* states, respectively, by the following choice of the coefficients:

$$c_{nr}^u = \frac{\alpha \sqrt{n+1}}{\sqrt{(n+1)\alpha^2 + \left(\left(\frac{1}{2} - \beta\right) - \sqrt{d_r}\right)^2}},$$

$$c_{nr}^d = \frac{\left(\frac{1}{2} - \beta - \sqrt{d_r}\right)}{\sqrt{(n+1)\alpha^2 + \left(\left(\frac{1}{2} - \beta\right) - \sqrt{d_r}\right)^2}}, \quad (6)$$

for the *right* states and

$$\begin{aligned} c_{nl}^u &= \frac{\alpha\sqrt{n}}{\sqrt{n\alpha^2 + \left(\left(\frac{1}{2} - \beta\right) + \sqrt{d_l}\right)^2}}, \\ c_{nl}^d &= \frac{\left(\frac{1}{2} - \beta + \sqrt{d_l}\right)}{\sqrt{n\alpha^2 + \left(\left(\frac{1}{2} - \beta\right) + \sqrt{d_l}\right)^2}}, \end{aligned} \quad (7)$$

for *left* states with $d_r = \sqrt{(n+1)\alpha^2 + \left(\frac{1}{2} - \beta\right)^2}$ and $d_l = \sqrt{n\alpha^2 + \left(\frac{1}{2} - \beta\right)^2}$. The energy eigenvalues of these states are

$$E_{nr} = \hbar\omega_c \left(1 + n - \sqrt{(n+1)\alpha^2 + \left(\frac{1}{2} - \beta\right)^2} \right), \quad (8)$$

$$E_{nl} = \hbar\omega_c \left(n + \sqrt{n\alpha^2 + \left(\frac{1}{2} - \beta\right)^2} \right). \quad (9)$$

In the following we use the notation

$$|n, \kappa\rangle = \sum_{\sigma} c_{n\kappa}^{\sigma} |n - \frac{\sigma - \kappa}{2}, \sigma\rangle. \quad (10)$$

where σ denotes the spin quantized in z -direction (1: *up*, -1: *down*) and κ the helicity (1: *right*, -1: *left*).

The low temperature magnetoconductivity is determined by the electron states close to the Fermi energy. We will be interested mainly in the low-magnetic field regime where the conductivity is dominated by contributions from Landau levels with $n \gg 1$ and we may simplify the energy spectrum by replacing $\alpha \rightarrow \bar{\alpha}/\sqrt{a^\dagger a + \frac{1}{2}}$ with $\bar{\alpha} = \frac{\alpha_z}{2\hbar\omega_c}$. With the approximation $\frac{n+1}{n} \rightarrow 1$ we arrive at a model with constant spin-splitting $\Delta_{SO} = 2\bar{\alpha}_z$ and the coefficients of (6) and (7) take the forms

$$\begin{aligned} c_r^u &= \frac{\bar{\alpha}}{\sqrt{\bar{\alpha}^2 + \left(\left(\frac{1}{2} - \beta\right) - \sqrt{d}\right)^2}}, \\ c_r^d &= \frac{\left(\frac{1}{2} - \beta - \sqrt{d}\right)}{\sqrt{\bar{\alpha}^2 + \left(\left(\frac{1}{2} - \beta\right) - \sqrt{d}\right)^2}} \end{aligned} \quad (11)$$

and

$$\begin{aligned} c_l^u &= \frac{\bar{\alpha}}{\sqrt{\bar{\alpha}^2 + \left(\left(\frac{1}{2} - \beta\right) + \sqrt{d}\right)^2}}, \\ c_l^d &= \frac{\left(\frac{1}{2} - \beta + \sqrt{d}\right)}{\sqrt{\bar{\alpha}^2 + \left(\left(\frac{1}{2} - \beta\right) + \sqrt{d}\right)^2}} \end{aligned} \quad (12)$$

respectively, where $\bar{d} = \sqrt{\bar{\alpha}^2 + \left(\frac{1}{2} - \beta\right)^2}$. For this constant SO coupling model the energy eigenvalues are

$$E_{nr} = \hbar\omega_c \left(1 + n - \sqrt{\bar{\alpha}^2 + \left(\frac{1}{2} - \beta\right)^2} \right), \quad (13)$$

$$E_{nl} = \hbar\omega_c \left(n + \sqrt{\bar{\alpha}^2 + \left(\frac{1}{2} - \beta\right)^2} \right). \quad (14)$$

The energy spectrum of this model (Fig. 1c) consists of the two branches of *right* and *left* states which by our choice of $\bar{\alpha}_z$ are shifted by $\Delta_{SO} = 5$ meV. The crossing of Landau levels takes place for all levels at the same magnetic field. Thus our model preserves the two main effects of SO coupling, the crossing of Landau levels and the mixing of spin components *up/down*.

III. SCBA WITH SPIN-DEGREE OF FREEDOM

For the calculation of the conductivity scattering has to be taken into account. The impurity-averaged Green function of the system G is given by the Dyson equation

$$G = G_0 + G_0 \Sigma G. \quad (15)$$

The scattering is included by the selfenergy Σ in self-consistent Born approximation (SCBA)²⁸. The matrix-elements of the selfenergy $\langle \alpha | \Sigma | \alpha' \rangle = \Sigma_{\alpha\alpha'}$, $\alpha = (n\kappa)$ read in the basis of eigenstates (10)

$$\Sigma_{\alpha\alpha'} = \sum_{\beta\beta'} \Gamma_{\alpha\beta\beta'\alpha'} G_{\beta\beta'}. \quad (16)$$

The kernel $\Gamma_{\alpha\beta\beta'\alpha'}$ is given by the expression

$$\Gamma_{\alpha\beta\beta'\alpha'} = \int \frac{dq^2}{(2\pi)^2} |\tilde{v}_I(\mathbf{q})|^2 \langle \alpha | e^{i\mathbf{q}\mathbf{r}} | \beta \rangle \langle \beta' | e^{-i\mathbf{q}\mathbf{r}} | \alpha' \rangle, \quad (17)$$

where $\tilde{v}_I(\mathbf{q})$ denotes the Fourier transform of the impurity potential²⁹.

We consider spin-conserving short range impurity scattering. By this choice we neglect magnetic impurities and SO coupling with the scattering center, thus without Rashba SO coupling scattering is possible only between states with the same spin-quantum number. In the new basis (10), including the Rashba term, scattering between states with different helicity becomes possible. For δ -scatterers Eq. (17) simplifies to

$$\begin{aligned} \Gamma_{\alpha\beta\beta'\alpha'} &= \Gamma^2 \sum_{\sigma\sigma'} (c_{n\kappa}^{\sigma})^* c_{m\bar{\kappa}}^{\sigma} (c_{m'\bar{\kappa}'}^{\sigma'})^* c_{n'\kappa'}^{\sigma'} \times \\ &\times \delta_{n - \frac{\sigma - \kappa}{2}, n' - \frac{\sigma' - \kappa'}{2}} \cdot \delta_{m - \frac{\sigma - \bar{\kappa}}{2}, m' - \frac{\sigma' - \bar{\kappa}'}{2}}, \end{aligned} \quad (18)$$

where $\Gamma^2 = \frac{1}{2\pi} \hbar\omega_c \frac{\hbar}{\tau}$ is connected through the relaxation time τ with the mobility $\mu = e\tau/m^*$ in the case without magnetic field. The Kronecker symbols have the form $\delta_{n', n-\theta}$ and $\delta_{m', m-\mu}$ with $\theta = \frac{1}{2}(\sigma - \sigma' - \kappa + \kappa') = -2, -1, 0, 1, 2$ and $\mu = \frac{1}{2}(\sigma - \sigma' - \bar{\kappa} + \bar{\kappa}') = -2, -1, 0, 1, 2$. We restrict ourselves to the diagonal approximation in the spacial quantum numbers by considering only $\theta = \mu = 0$. In this approximation the selfenergy reads $\Sigma_{nn'}^{\kappa\kappa'} = \Sigma^{\kappa\kappa'} \delta_{nn'}$ with $\Sigma^{\kappa\kappa'}$ independent of n , and the Green function $G_{mm'}^{\kappa\kappa'} = G_m^{\kappa\kappa'} \delta_{mm'}$. Thus the SCBA self-energy becomes

$$\Sigma^{\kappa\kappa'} = \Gamma^2 \sum_m \sum_{\bar{\kappa}\bar{\kappa}'} \alpha_{\bar{\kappa}\bar{\kappa}'}^{\kappa\kappa'} G_m^{\bar{\kappa}\bar{\kappa}'} \quad (20)$$

with

$$\alpha_{\kappa\bar{\kappa}'}^{\kappa\kappa'} = \sum_{\sigma\sigma'} (c_{\kappa}^{\sigma})^* c_{\bar{\kappa}}^{\sigma} (c_{\bar{\kappa}'}^{\sigma'})^* c_{\kappa'}^{\sigma'} \delta_{\sigma-\sigma', \kappa-\kappa'} \delta_{\sigma-\sigma', \bar{\kappa}-\bar{\kappa}'} \quad (21)$$

and

$$\left(G_m^{\kappa\kappa'}\right)^{-1} = \left(G_0^{\kappa}\right)^{-1} \delta_{\kappa\kappa'} - \Sigma^{\kappa\kappa'}, \quad (22)$$

where G_0^{κ} is the Green function of the system without impurities. Using the abbreviations $\Sigma^{\kappa\kappa} \equiv \Sigma^{\kappa}$, $G_m^{\kappa\kappa} \equiv G_m^{\kappa}$ and $\alpha_{\kappa\bar{\kappa}'}^{\kappa\kappa} \equiv \alpha_{\kappa\bar{\kappa}'} \delta_{\kappa\bar{\kappa}'}$ the selfenergy can now be calculated from

$$\Sigma^{\kappa} = \Gamma^2 \sum_{m\bar{m}} \alpha_{\kappa\bar{m}} G_m^{\bar{m}} \quad \text{with} \quad \alpha_{\kappa\bar{m}} = \sum_{\sigma} |c_{\kappa}^{\sigma}|^2 |c_{\bar{m}}^{\sigma}|^2. \quad (23)$$

The off-diagonal elements of the selfenergy will be neglected.

The density of states for the *left* and *right* components are obtained by the trace over the spectral functions $A_m^{\kappa} = -\text{Im} \left\{ \frac{1}{\pi} G_m^{\kappa} \right\}$.

$$\begin{aligned} D^{\kappa}(E) &= \frac{1}{L_x L_y} \text{Tr}_m \{ A_m^{\kappa} \} = \\ &= -\frac{1}{(\pi \lambda_c \Gamma)^2} \sum_{\kappa'} (\alpha^{-1})_{\kappa\kappa'} \text{Im} \left\{ \Sigma^{\kappa'}(E) \right\}. \end{aligned} \quad (24)$$

Here $(\alpha^{-1})_{\kappa\kappa'}$ is the inverse of the matrix formed from the $\alpha_{\kappa\kappa'}$ of Eq. (23) for which $\alpha_{\kappa\kappa} + \alpha_{\kappa(-\kappa)} = 1$. For vanishing SO coupling one has $\alpha_{\kappa\bar{\kappa}} \rightarrow \delta_{\kappa\bar{\kappa}}$ and the standard SCBA result is reproduced. For strong SO coupling if $\bar{\alpha} > 1$, i.e. the Landau splitting is smaller than the splitting induced by the SO interaction, one has $\alpha_{\kappa\bar{\kappa}} \rightarrow \frac{1}{2}$.

Due to the SO interaction the Landau levels of different helicity cross as seen in Fig. 1b and c. To demonstrate the influence of scattering around these crossing points we apply the described extension of the SCBA to a two level system with different spacings. The two states at the energies E_r, E_l have different helicity and evolve with increasing SO coupling from the spin *up/down* states with energy E_u and E_d .

In Fig. 2a the situation without SO interaction $\alpha_{\kappa\bar{\kappa}} = \delta_{\kappa\bar{\kappa}}$ is shown. For decreasing energy difference $E_u - E_d$ the form of the selfenergy, calculated from Eq. (23), and the density of states, from Eq. (24), keeps unchanged. In contrast, in the case of SO coupled states (Fig. 2b, with $\alpha_{\kappa\kappa} = 0.6$) the impurity scattering adds to the selfenergy a contribution at the neighbouring state with opposite helicity. If the states are not degenerate, both width and height of the imaginary part of the selfenergy are reduced as compared with Fig. 2a, while for the degenerate levels the selfenergy and the density of states are identical with the situation of pure spin states. For strongly SO coupled states $\alpha_{\kappa\kappa} \rightarrow \frac{1}{2}$ the height and width of the imaginary part of the selfenergy are reduced by $1/\sqrt{2}$, as can be seen from Eq. (23). As these parameters are inversely proportional to the relaxation time we conclude, that the

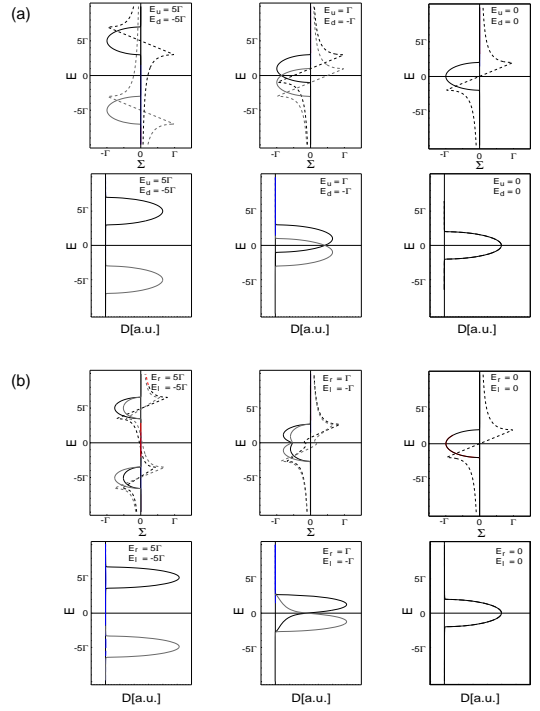


FIG. 2: Selfenergies $\Sigma(E)$ and density of states for a two-level system without (a) and with (b) SO coupling for different separation of the up-/down- or right-/left-eigenstates in (a) and (b), respectively. In (b) a mixing coefficient $\alpha_{\kappa\kappa} = 0.6$ at the energies E_r and E_l has been chosen.

scattering time is increased by the SO coupling, away from the crossing points.

To summarize, the scattering strength depends on the level separation, i.e. on the distance from crossing points in Fig. 1. As this distance varies with the magnetic field we expect a modulation of the scattering strength with the magnetic field.

IV. CONDUCTIVITY

Based on the exact eigenstates of the constant SO coupling model we evaluate the Kubo formula

$$\sigma_{\mu\mu} = \frac{e^2 \pi \hbar}{L_x L_y} \int dE \left(-\frac{df_0}{dE} \right) \sum_{\alpha\alpha'} |\langle \alpha | v_{\mu} | \alpha' \rangle|^2 A_{\alpha} A_{\alpha'} \quad (25)$$

to calculate the conductivity. Here the spectral function A_{α} includes the impurity scattering in SCBA as described in Sec. III and the Fermi distribution function yields the temperature average. The velocity is given by the equation $i\hbar v_{\mu} = [x_{\mu}, H]$, which results in

$$v_x = \frac{1}{m^*} \left(\pi_x + \frac{\alpha_z}{\hbar} \sigma_y \right) \quad \text{and} \quad v_y = \frac{1}{m^*} \left(\pi_y - \frac{\alpha_z}{\hbar} \sigma_x \right). \quad (26)$$

Besides $\sigma_{\mu\mu}, \mu = x, y$ we calculate also the thermodynamic density of states at the Fermi energy $D_F =$

$\int dE(-\frac{df_0}{dE})D(E)$. In Fig. 3 both quantities are shown for the two temperatures $T = 1\text{ K}$ and $T = 3\text{ K}$ with the Fermi energy determined from the constant electron density n_s . For comparison the classical high temperature limit of the SCBA for decoupled Landau levels is given by the dashed line. The effect of spin-orbit

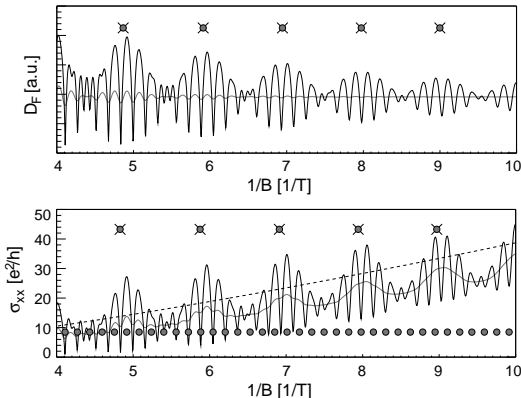


FIG. 3: Thermodynamic density of states at the Fermi energy D_F and longitudinal conductivity σ_{xx} for the parameters of Fig. 1, electron density $n_s = 3.0 \times 10^{15} \text{ m}^{-2}$ and mobility $\mu = 50 \text{ m}^2/\text{Vs}$ at two temperatures $T = 1.0\text{ K}$ (black solid) and 3.0 K (grey solid). The grey circless mark the expected position of maxima of the SdH oscillations without SO coupling; Landau level crossings due to the SO coupling are indicated by crosses. The dashed line in the plot of the longitudinal conductivity is the classical limit of the SCBA when the Landau levels are decoupled.

pling is seen in D_F as the beating pattern, well-known from measured SdH oscillations^{14,15,16,17}, while in σ_{xx} it causes an additional modulation, which survives even at a higher temperature when the SdH oscillations are damped out. The period of this modulation is determined by the crossing of Landau levels (marked in Fig. 3) induced by the spin-orbit coupling. The self-energy enters differently into D_F and σ_{xx} . In D_F it leads to a modulated broadening of the Landau levels which is washed out in the high-temperature limit, while in σ_{xx} it acts in addition as a scattering time whose dependence on the level separation remains even at higher temperatures. This is seen by comparing with the classical SCBA limit for decoupled Landau levels (dashed lines): the Kubo formula (25) yields a magnetoconductivity which is reduced away from the crossing points due to suppression of impurity scattering. (Note, that we are in the limit $\omega_c\tau \gg 1$, where the Drude conductivity is proportional to $1/\tau$.) To demonstrate the effect of scattering between states of different helicity in our extension of the SCBA, we show in Fig. 4 the dependence of the conductivity at $T = 3\text{ K}$ on the mixing coefficient $\alpha_{\kappa\tilde{\kappa}}$ by keeping the energy spectrum with spin-orbit splitting unchanged but varying $\alpha_{\kappa\kappa}$, which otherwise is given by the coefficients c_{κ}^{σ} . Neglecting the scattering between states of different helicity $\alpha_{\kappa\kappa} = 1$, the crossing of Landau levels has no effect on the conductivity. For dominant spin-

orbit coupling, $\alpha_{\kappa\kappa} \rightarrow \frac{1}{2}$, we see that the conductivity is reduced between crossing points of Landau levels. We can distinguish two situations (top of Fig. 4): The states with different helicity are degenerate (A) and the scattering efficiency keeps unchanged; When *right/left*-states are not degenerate (B) the conductivity depends on $\alpha_{\kappa\tilde{\kappa}}$.

In Fig. 5, we have varied the strength of the impurity

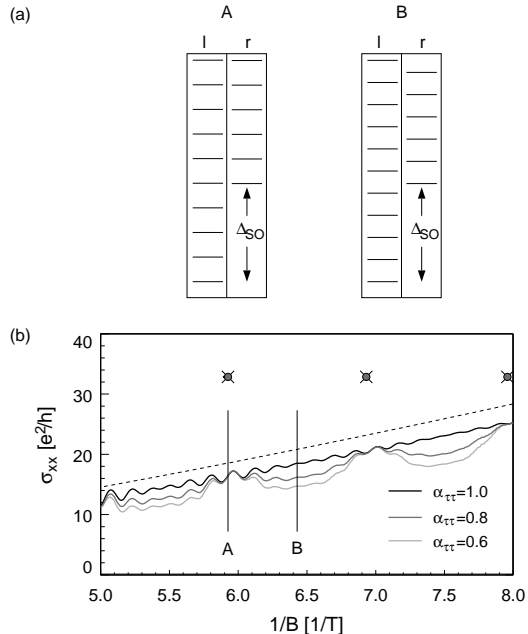


FIG. 4: (a) Sketch of Landau level spectrum with (A) and without (B) degeneracy of states with different helicity. (b) Longitudinal magnetoconductivity in dependence of the strength of the SO coupling expressed by the parameter $\alpha_{\kappa\kappa}$ for high temperature $T = 3.0\text{ K}$. The parameters are those of Fig. 3 and the dashed line is again the classical limit of the SCBA when the Landau levels are decoupled.

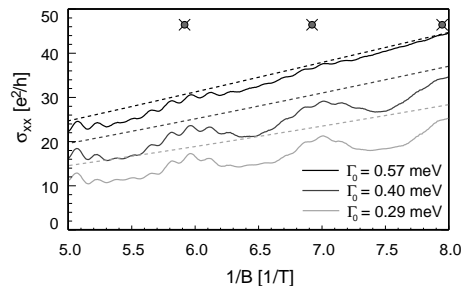


FIG. 5: Longitudinal magnetoconductivity at fixed $\alpha_{rr} = 0.6$ but with different Γ_0 at $T = 3.0\text{ K}$. The other parameters are those of Fig. 3. The dashed lines mark the classical limit of the SCBA with decoupled Landau levels.

scattering by changing the parameter Γ . At the classical limit of the SCBA with decoupled Landau levels (dashed lines), we see that the conductivity rises with increasing Γ . The modulation of the conductivity due to the crossing of Landau levels decreases, because the limit

of decoupled Landau levels cannot be reached for large enough Γ .

We have shown by a quantum mechanical calculation, that the SO coupling causes the expected beats of the SdH oscillations. In addition our results exhibit a new modulation of the magnetoconductivity which can be ascribed to a modification of impurity scattering in the presence of SO coupling. This could help in experiments to distinguish the effect of the SO coupling from that of inhomogeneous electron densities which was invoked in Ref.²⁰ to explain beatings in the SdH oscillations.

V. MAGNETOTRANSPORT IN LATERAL SUPERLATTICES WITH SPIN-ORBIT COUPLING

Lateral semiconductor superlattices have proven to be well suited for studying the physics of Bloch electrons in artificial periodic systems²¹. A variety of oscillations have been observed in magnetotransport experiments for systems, in which the lattice constant a is comparable with achievable magnetic lengths $\lambda_c = \sqrt{\frac{\hbar}{eB}}$ and both being much smaller (at low temperature) than the carrier mean-free-path. After having studied the SdH oscillations in the previous section we focus here on the influence of the Rashba SO interaction on the various magnetoconductivity oscillations due to the periodic modulation mentioned in the introduction. For the lateral superlattice with Rashba SO interaction the Hamiltonian is given by

$$H = \begin{pmatrix} \frac{1}{2m^*}(\pi_x^2 + \pi_y^2) & \frac{\alpha_z}{\hbar}(\pi_x + i\pi_y) \\ \frac{\alpha_z}{\hbar}(\pi_x - i\pi_y) & \frac{1}{2m^*}(\pi_x^2 + \pi_y^2) \end{pmatrix} + \begin{pmatrix} V(x, y) & 0 \\ 0 & V(x, y) \end{pmatrix}. \quad (27)$$

We consider here a periodic modulation in x direction described by

$$V(x) = \frac{V_0}{2} \cos\left(\frac{2\pi}{a}x\right). \quad (28)$$

It removes the degeneracy of the Landau levels and is taken into account in evaluating the Kubo formula together with the spin-conserving impurity scattering in the extension of the SCBA as for the homogeneous 2DES. In Fig. 6 the longitudinal magnetoconductivities σ_{xx} and σ_{yy} , in the direction of the modulation and perpendicular to it, respectively, are depicted for potential parameters $V_0 = 3$ meV, $a = 75$ nm, and two temperatures. The Fermi energy was fixed to $E_F = 30$ meV, much larger than the amplitude of the periodic potential, which defines the weak modulation case. The mixing coefficient was fixed to the maximum value $\alpha_{\kappa\kappa} = \frac{1}{2}$. Different types of oscillations can be identified of which at the higher temperature (3 K) only the commensurability oscillations and the modulation due to SO coupling survive. The periods (seen in the 1 K traces) can be quantified in simplified models. Following Onsager³² the SdH periods

are

$$\Delta_{1/B}^{\text{SdH:}+/-} = \frac{e\hbar}{m^*(E_F \pm \frac{1}{2}\Delta_{\text{SO}})}, \quad (29)$$

where the appearance of two Fermi contours due to the spin-splitting is accounted for¹⁹. The period of the commensurability oscillations is given by²⁶

$$\Delta_{1/B}^{\text{CO:}+/-} = \frac{ea}{2\sqrt{2m^*(E_F \pm \frac{1}{2}\Delta_{\text{SO}})}}. \quad (30)$$

where again the spin-split Fermi contours are considered. The periods reflecting the formation of the miniband structure due to the periodic potential^{24,30,31} are quantified by

$$\Delta_{1/B} = \frac{2\pi e}{\hbar} \frac{1}{A}, \quad (31)$$

where A is the cross section of the modified Fermi contour given in Ref.³¹. Again the spin-splitting due to SO coupling is to be considered and Eq. (31) yield two periods for the Fermi cross sections

$$A^{\text{1D:}+/-} = \frac{2m^*(E_F \pm \frac{1}{2}\Delta_{\text{SO}})\pi}{\hbar^2} - 2\left(\frac{\pi}{a}\right) \sqrt{\frac{2m^*(E_F \pm \frac{1}{2}\Delta_{\text{SO}})}{\hbar^2} - \left(\frac{\pi}{a}\right)^2} - \frac{4m^*(E_F \pm \frac{1}{2}\Delta_{\text{SO}})}{\hbar^2} \arcsin \frac{\pi\hbar}{a\sqrt{2m^*(E_F \pm \frac{1}{2}\Delta_{\text{SO}})}}. \quad (32)$$

Finally we may conclude from the eigenvalues of Eq. (8) for $n \gg 1$ a period of

$$\Delta_{1/B}^{\text{SO}} = \frac{e\hbar}{m^*\Delta_{\text{SO}}} \quad (34)$$

for the modulation connected with the crossing points of the Landau levels at the Fermi energy.

In order to analyze all these oscillations we take the power spectrum of the differences $\Delta\sigma_{\mu\mu}$, $\mu = x, y$, of the calculated longitudinal conductivities at 1 and 8 K. It is shown in dependence on the strength of the SO coupling (Fig. 7) and on the Fermi energy E_F (Fig. 8) together with the periods predicted from Eqs. (29)-(34). In Fig. 7 we see that with increasing SO coupling the frequencies of all (but one) resolved $1/B$ periodic oscillations split and the maxima of the Fourier transform follow the predictions of the simplified models. This is not the case for the peaks showing up at the lowest $f_{1/B}$ values. These peaks, being due to the modulation resulting from our extension of the SCBA (Sec. III), do not split and follow the analytic expressions of Eq. (34). In Fig. 8 the oscillation period is shown in dependence on the Fermi energy. Again the maxima of our full quantum-mechanical calculation follow the predictions of the simplified models of Eqs. (29)-(34).

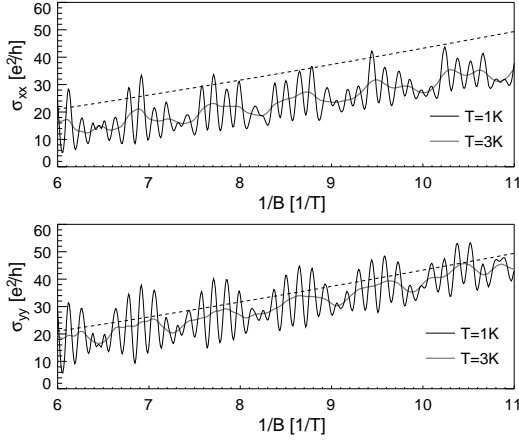


FIG. 6: Longitudinal magnetoconductivities σ_{xx} and σ_{yy} for a lateral superlattice with uni-directional modulation in x -direction. (modulation amplitude $V_0 = 3$ meV, lattice constant $a = 75$ nm, Fermi energy $E_F = 30$ meV, mobility $\mu = 50$ m²/Vs and InAs effective mass $m^* = 0.0229 m_e$. The SO coupling is $\alpha_z = 2.0 \times 10^{-11}$ eVm and the mixing coefficient $\alpha_{\kappa\kappa} = 0.5$.

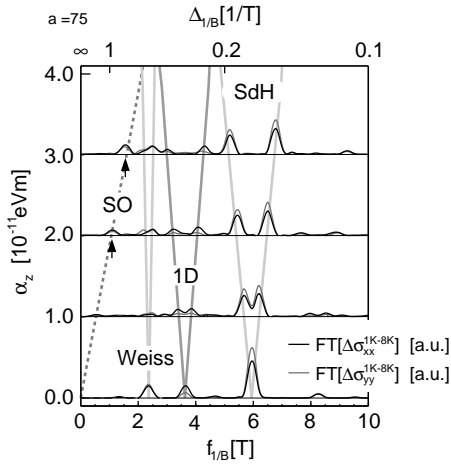


FIG. 7: The absolute value of the Fourier spectrum of the difference of the conductivities at 1 K and 8 K analogous to Fig. 6 is shown in dependence on α_z . The arrows mark the contribution due to the crossing of Landau levels. The calculated Fourier spectrum is compared with the models of Eqs. (29),(30), (31) and (34).

VI. SUMMARY

We have calculated the magnetoconductivity for a homogenous 2DES with spin-orbit interaction including a non-trivial extension of the SCBA which takes into account the spin-degree of freedom. The crossing of Lan-

da levels with different helicity, which is induced by the spin-orbit interaction, manifests itself in an additional modulation of the conductivity. It is due to a modification of impurity scattering in the presence of SO coupling. This signature could be used - besides the beating

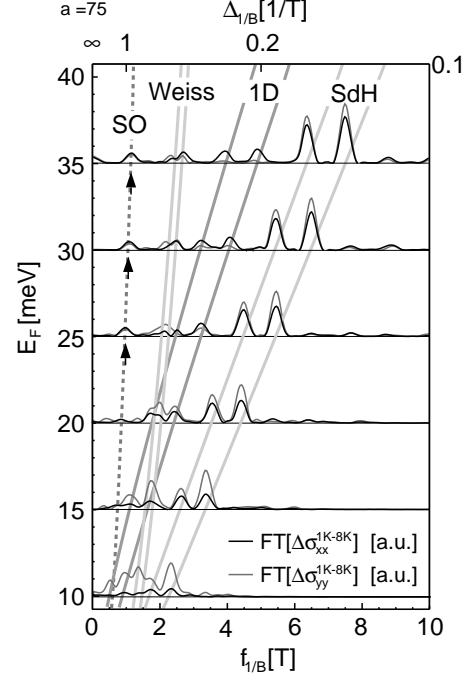


FIG. 8: The absolute value of the Fourier spectrum of the difference of the conductivities at 1 K and 8 K analogous to Fig. 6 is shown in dependence on the Fermi energy E_F . The arrows mark the contribution due to the crossing of Landau levels. Comparison with Eqs. (29),(30), (31) and (34) is shown by straight lines.

of SdH oscillations - for the experimental verification of SO coupling.

Further we have investigated the influence of SO interaction on the magnetoconductivity oscillations in 1D lateral superlattices. The prediction of the frequencies by simple models and the numerical calculations are in agreement and should motivate an experimental verification.

Acknowledgments

This work has been supported by the DFG via Forschergruppe 370 *Ferromagnet-Halbleiter-Nanostrukturen*.

* Electronic address: michael.langenbuch@physik.uni-regensburg.de
 † Fraunhofer Institut Naturwissenschaftlich-Technische Trendanalysen, Appelsgarten 2, 53879 Euskirchen, Germany

- ¹ É.I. Rashba, *Sov. Phys. Sol. Stat.* **2**, 1109 (1960).
- ² Yu.A. Bychkov and É.I. Rashba, *JETP Lett.* **39**, 78 (1984).
- ³ S.A. Wolf, D.D. Awschalom, R.A. Buhrman, J.M. Daughton, S. von Molnár, M.L. Roukes, A.Y. Chtchelkanova, D.M. Treger, *Science* **294**, 1488 (2001).
- ⁴ G. Dresselhaus, *Phys. Rev.* **100**, 580 (1955).
- ⁵ L. Wissinger, U. Rössler, R. Winkler, B. Jusserand, and D. Richards, *Phys. Rev. B* **58**, 15375 (1998).
- ⁶ F.G. Pikus and G.E. Pikus, *Phys. Rev. B* **51**, 16928 (1995).
- ⁷ Ch. Schierholz, R. Kürsten, G. Meier, T. Matsuyama, and U. Merkt, *phys. stat. sol. (b)* **233**, 436 (2002).
- ⁸ G.E. Pikus, A.N. Titkov in: *Optical Orientation*, edited by F. Meier and B.P. Zakharchenya, North-Holland, Amsterdam (1984).
- ⁹ M.I. Dyakonov and V.I. Perel, *Sov. Phys. Solid State* **13**, 3023 (1972).
- ¹⁰ N.S. Averkiev and L.E. Golub, *Phys. Rev. B* **60**, 15582 (1999).
- ¹¹ J. Kainz, U. Rössler, and R. Winkler, *cond-mat/0304017* (2003).
- ¹² S.D. Ganichev, S.N. Danilov, V.V. Bel'kov, E.L. Ivchenko, M. Bichler, W. Wegscheider, D. Weiss, and W. Prettl, *Phys. Rev. Lett.* **88**, 057401 (2002).
- ¹³ G. Lommer, F. Malcher and U. Rössler, *Phys. Rev. Lett.* **60**, 728 (1988).
- ¹⁴ J. Nitta, T. Akazaki, H. Takayanagi, T. Enoki, *Phys. Rev. Lett.* **78**, 1335 (1997).
- ¹⁵ J.P. Heida, B.J. van Wees, J.J. Kuipers, and T.M. Klapwijk, G. Borghs, *Phys. Rev. B* **57**, 11911 (1998).
- ¹⁶ Th. Schäpers, G. Engels, J. Lange, Th. Klocke, M. Hollfelder, and H. Lüth, *J. Appl. Phys.* **98**, 4324 (1998).
- ¹⁷ C.-M. Hu, J. Nitta, T. Akazaki, H. Takayanagai, J. Osaka, P. Pfeffer, W. Zawadzki, *Phys. Rev. B* **60**, 7736 (1999).
- ¹⁸ R. Winkler, S.J. Papadakis, E.P. De Poortere, and M. Shayegan, *Phys. Rev. Lett.* **84**, 713 (2000).
- ¹⁹ S. Keppeler, R. Winkler, *Phys. Rev. Lett.* **88**, 046401 (2002).
- ²⁰ S. Brosig, K. Ensslin, R. J. Warburton, C. Nguyen, B. Brar, M. Thomas, H. Kroemer, *Phys. Rev. B* **60**, R13989 (1999).
- ²¹ D. Weiss, *Adv. Sol. Stat. Phys.* **31**, 341 (1991).
- ²² D. Weiss, K. von Klitzing, K. Ploog, and G. Weimann, *Europhys. Lett.* **8**, 179 (1989); R.W. Winkler, J.P. Kotthaus, and K. Ploog, *Phys. Rev. Lett.* **62**, 1177 (1989).
- ²³ C. Albrecht, et al., *Phys. Rev. Lett.* **83**, 2234 (1999).
- ²⁴ R.A. Deutschmann, W. Wegscheider, M. Rother, M. Bichler, G. Abstreiter, C. Albrecht, J.H. Smet, *Phys. Rev. Lett.* **86**, 1857 (2001).
- ²⁵ M. Langenbuch, M. Suhrke, U. Rössler, *Proceedings 2nd PASPS Würzburg*, accepted for publication in *Journal of Superconductivity* (2002).
- ²⁶ L.L. Magarill, *Superlattices and Microstructures* **16**, 257 (1994).
- ²⁷ D. Weiss, K. von Klitzing, K. Ploog, and G. Weimann, *Europhys. Lett.* **8**, 179 (1989); R.W. Winkler, J.P. Kotthaus and K. Ploog, *Phys. Rev. Lett.* **62**, 1177 (1989).
- ²⁸ T. Ando, A.B. Fowler and F. Stern, *Reviews of Modern Physics* **54**, 437 (1982).
- ²⁹ R.R. Gerhardtts, *Zeitschrift für Physik B* **22**, 327 (1975).
- ³⁰ C. Albrecht, J.H. Smet, D. Weiss, K. von Klitzing, V. Umansky, H. Schweizer, *Physica B* **249-251**, 914 (1998).
- ³¹ M. Langenbuch, R. Hennig, M. Suhrke, U. Rössler, C. Albrecht, J.H. Smet, D. Weiss, *Physica E* **6**, 565 (2000).
- ³² L. Onsager, *Phys. Rev.* **37**, 405 (1931).